A polydiacetylene–nested porphyrin conjugate for dye-sensitized solar cells†

Nuttapol Pootrakulchote,[a] Chawanwit Reanprayoon,[b] Jacek Gasiorowski,[c] Niyazi Serdar Sariciftci[c] and Patchanita Thamyongkit*[d]

A polydiacetylene (PDA)–nested zinc-porphyrin derivative was prepared and investigated for its potential applicability in dye-sensitized solar cells (DSSCs). Absorption enhancement at 525–625 nm was observed as a proof of successful PDA formation. Cyclic voltammetry analysis suggested the appropriate positions of the highest occupied molecular orbital (HOMO) and the lowest unoccupied molecular orbital (LUMO) energy levels of the target material for DSSCs. Optimum DSSCs based on the PDA–nested zinc-porphyrin exhibited a short-circuit photocurrent density (J_{sc}), an open-circuit voltage (V_{oc}) and a fill factor (FF) of 4.2 mA cm^{-2}, 0.7 V and 0.78, respectively, with an overall power conversion efficiency (PCE) of 2.3%. The photovoltage decay analysis also indicated that the electron recombination lifetime of the cells was prolonged as a result of the presence of the PDA-containing C_{25} alkyl chains in the porphyrin dye system.

Introduction

Porphyrins are attractive materials due to their adjustable photophysical and electrochemical properties *via* modification of peripheral substituents and central metals,[1] as well as thermal- and photostability. Up to date, several porphyrinic derivatives have been proposed for being used as key constituents in (opto)electronic devices, such as photovoltaic cells,[2] organic light-emitting diodes (OLEDs),[3] and organic field-effect transistors (OFETs).[4] Recently, they have proven to be promising candidates for dye-sensitized and bulk-heterojunction solar cells (DSSCs[5] and BHJ-SCs,[6] respectively).

Our recent work reported the synthesis and use of polydiacetylene (PDA)–nested zinc-porphyrin for the BHJ-SCs, showing that the presence of a PDA network significantly enhanced the absorption of the porphyrin at the region of 530–600 nm and suggesting the potential use as an electron donating material in the BHJ-SCs.[7] The objective of this work is to explore the

possibility of using a novel PDA–nested zinc-porphyrin derivative as a dye in the DSSCs. The porphyrin monomer contains three *meso*-C_{25} alkyl chains having diacetylene (DA) units, which can be photopolymerized to give a porphyrin embedded PDA web, and one carboxyl anchoring group at the remaining *meso* position of the porphyrin. According to previous studies,[7,8] this system is designed with three main advantages: (i) π-stacking of the porphyrin macrocycle can facilitate the local orientation of the DA units for the desirable photopolymerization, (ii) the long chain of the DA-containing C_{25} alkyl chains can serve as solubilizing groups in organic solvents, and (iii) the formation of the PDA network can enhance the absorption at 500–650 nm, where the porphyrin has low absorptivity. To the best of our knowledge, PDA was previously studied as a hole transport material in solid state DSSCs by Wang *et al.*,[9] but a porphyrin–PDA conjugate has not been investigated for use in the DSSCs. In this work, we report the novel PDA–nested zinc-porphyrin conjugate exhibiting suitable photophysical and electrochemical properties for DSSC applications, and giving favorable device performance. The results from these studies will become a useful guideline for the development of other porphyrin-based and PDA-based materials for optoelectronic applications.

[a] *Department of Chemical Technology, Faculty of Science, Chulalongkorn University, Bangkok 10330, Thailand*

[b] *Program in Petrochemistry and Polymer Science, Faculty of Science, Chulalongkorn University, Bangkok 10330, Thailand*

[c] *Linz Institute for Organic Solar Cells (LIOS), Institute of Physical Chemistry, Johannes Kepler University Linz, Linz 4040, Austria*

[d] *Department of Chemistry, Faculty of Science, Chulalongkorn University, Bangkok 10330, Thailand. E-mail: patchanita.v@chula.ac.th; Fax: +662-254-1309; Tel: +662-218-7587*

† Electronic supplementary information (ESI) available: Spectral data, including the ¹H-NMR spectrum, ¹³C-NMR spectrum and mass spectra of new compounds. See DOI: 10.1039/c5nj01583a

Experimental

Materials and methods

All chemicals were of analytical grade, purchased from commercial suppliers and used as received without further purification. ¹H-NMR and ¹³C-NMR spectra were obtained in deuterated chloroform

(CDCl$_3$) using an NMR spectrometer operated at 400 megahertz (MHz) for ^{1}H and 100 MHz for ^{13}C nuclei. Chemical shifts (δ) are reported in parts per million (ppm) relative to the residual CHCl$_3$ peak (7.26 ppm for ^{1}H-NMR and 77.0 ppm for ^{13}C-NMR). Coupling constants (J) are reported in Hz. Mass spectra were obtained by matrix-assisted laser desorption ionization mass spectrometry (MALDI-MS) using dithranol as a matrix. Absorption and emission spectra of dye solutions were measured in toluene at room temperature. Absorption data of a film of porphyrin–PDA conjugate were collected from the film prepared by submerging a TiO$_2$ film into a 0.3 mM monomer solution in a mixed solvent of tetrahydrofuran (THF) and ethanol (v/v, 1/4) at room temperature for 16 h, followed by exposing the resulting dry film under ambient light for at least 1 h or under a 254 nm ultraviolet radiation for 15 min.

Non-commercial compounds. 5,10,15,20-Tetra(4-carboxyphenyl)-porphyrin (**1**)[10] and 1-amino-10,12-pentacosadiyne (**3**)[11] were prepared following literature procedures.

Synthesis of Zn-4. Following a previously published procedure[12] with slight modification, compound **1** (0.134 g, 0.170 mmol) was stirred in THF (10 mL) and *N*-hydroxysuccinimide (NHS) (0.128 g, 1.12 mmol, 6 equiv.) and 1-ethyl-3-(3-dimethylaminopropyl)-carbodiimide hydrochloride (EDC·HCl) (0.222 g, 1.16 mmol, 7 equiv.) were added. The reaction mixture was stirred at reflux temperature for 2 days and the solvent was then removed under reduced pressure. The resulting crude containing compound **2** was dissolved in THF (10 mL) and treated with compound **3** (0.565 g, 1.57 mmol, 9 equiv.) and triethylamine (TEA, 5 mL). The reaction mixture was stirred at reflux temperature for 1 d. After the solvent was removed under reduced pressure, the crude mixture was purified by column chromatography [silica, DCM : EtOH : TEA (96 : 3 : 1)]. Compound **4** (0.101 g) was obtained as a purple solid which was used in the Zn-metallation step without further purification. λ_{abs}/nm 419, 514, 548, 593, 648; λ_{em} (λ_{ex} = 419 nm)/nm 651, 712; MALDI-TOF-MS *m/z* obsd 1817.311 (M$^+$, 100), calcd 1815.622 (M = C$_{123}$H$_{159}$N$_7$O$_5$).

Following a previously published procedure,[13] a solution of compound **4** (0.101 g, 0.055 mmol) in chloroform (3 mL) was reacted with a solution of zinc acetate dihydrate (0.063 g, 0.29 mmol) in methanol (1 mL) at room temperature for 3 h. The resulting mixture was extracted with CH$_2$Cl$_2$ and H$_2$O. The organic phase was dried over anhydrous magnesium sulfate and concentrated to dryness. The resulting crude was purified by washing with hexane and then methanol to afford compound **Zn-4** as a purple solid (0.081 g, 25% from **1**). mp > 230 °C (from methanol); λ_{abs}/nm 425, 557, 598; λ_{em} (λ_{ex} = 425 nm)/nm 605, 651; ^{1}H NMR δ 0.89 (9 H, t, J = 7.3 Hz, CH$_3$), 1.10–1.80 (102 H, m, CH$_2$), 2.00–2.50 (12 H, m, CH$_2$), 3.00–3.50 (6 H, m, CH$_2$), 4.50–4.60 (1 H, m, NH), 5.20–5.50 (2 H, m, NH), 5.90–6.30 (4 H, m, CH), 7.50–7.75 (12 H, m, CH), 8.05–8.30 (6 H, m, CH), 8.80–8.90 (2 H, m, CH); ^{13}C NMR δ 14.1, 19.2, 22.7, 25.5, 26.8, 26.9, 27.0, 28.3, 28.4, 28.7, 28.8, 28.9, 29.0, 29.1, 29.2, 29.3, 29.5, 29.6, 30.1, 31.9, 35.4, 35.9, 36.5, 36.7, 39.6, 40.2, 40.6, 62.7, 65.3, 127.1, 137.4, 158.5, 166.6, 171.9; MALDI-TOF-MS *m/z* obsd 1373.194 [(M-C$_{37}$H$_{63}$)$^+$, 45], 1881.103 [M$^+$, 55] calcd 1879.017 [M$^+$], (M = ZnC$_{123}$H$_{157}$N$_7$O$_5$).

Electrochemical studies. Following a reported procedure,[7] electrochemical characterization of **poly-Zn-4** was performed by cyclic voltammetry operating in the three electrode configuration. Acetonitrile containing 0.1 M Bu$_4$NPF$_6$ was used as an electrolyte solution, an indium tin oxide-coated glass (ITO/glass) covered with **poly-Zn-4** as a working electrode, a Pt foil as a counter electrode and a Ag/AgCl as a quasi-reference electrode (QRE). The **poly-Zn-4** film was prepared from the 254 nm ultraviolet radiation of a **Zn-4**-spincoated film on the ITO/glass at room temperature for 15 min. The QRE was externally calibrated with a ferrocene/ferrocenium redox couple of which the potential value of 0.40 V *vs.* NHE was used. All cyclic voltammetry measurements were performed with a scan rate of 20 mV s^{-1}.

Device fabrication and characterization. This study employed screen-printed TiO$_2$ particles as photoelectrodes. An 8 μm thick transparent film of 20 nm size TiO$_2$ was first printed on the fluorine doped SnO$_2$ (FTO) conducting glass electrode and then followed by a 5 μm thick second layer of 400 nm light scattering TiO$_2$ particles. The double layer TiO$_2$ film was sintered at 500 °C, cooled down to ∼80 °C, and then submerged into the dye solution (0.3 mM) using a mixed solvent of THF and ethanol (v/v, 1/4) for 16 h. The resulting dyed TiO$_2$ film was exposed to ambient light for at least 1 h to proceed the photopolymerization. To fabricate the devices, the stained photoanode was assembled with the platinized counter electrode using a 25 μm thick Surlyn hot melt ring (Dupont, USA) and sealed by heating press. The internal gap between two glasses was filled with a volatile liquid electrolyte (1.0 M 1,3-dimethylimidazolium iodide (DMII), 0.5 M *tert*-butylpyridine (tBP), 0.1 M guanidiniumthio-cyanate (GNCS), 0.1 M LiI and 0.03 M I$_2$ in the mixed solvent of acetonitrile and valeronitrile (v/v, 85/15)).

To characterize the DSSCs, a 450 W xenon light source (Oriel, USA) was used. The current density–voltage (J–V) characteristics were obtained by applying external potential bias to the cell and measuring the generated photocurrent using a Keithley model 2400 digital source meter (Keithley, USA). The devices were masked to attain an illuminated active area of 0.159 cm^2. Loss of light due to reflection from the photoanode glass was reduced by applying a self-adhesive fluorinated polymer anti-reflecting film (ARKTOP, Asahi glass). Up to four devices were fabricated for each experimental variable change to give accurate statistics. Detailed methods for the TiO$_2$ film preparation, the device fabrication and the current–voltage measurements are described elsewhere.[14]

A modulated light intensity data acquisition system was used to control the incident photon-to-current conversion efficiency (IPCE) measurement. The modulation frequency was about 1 Hz. Light from a 300 W Xenon lamp (ILC Technology, USA) was focused through a computer controlled Gemini-180 double monochromator (JobinYvon Ltd, UK) onto the photo-voltaic cell. White light bias was used to bring the total light intensity on the device closer to operating conditions.

In the transient photoelectrical decay experiments, different steady-state light levels were provided by a homemade white light-emitting diode array tuning the driving voltage. A red light-emitting diode array controlled with a fast solid-state

switch was used to generate a perturbation pulse of 50 ms duration. The pulsed red- and steady-state white-light were both incident on the working electrode side of the test cell. The intensity of the red light pulse was carefully controlled by the driving potential of the red diode array to keep the modulated photovoltage below 10 mV. In a transient photovoltage decay measurement, the cells were maintained at open circuit voltage under the white light and the transient photovoltage decay following the red light pulse was monitored. Normally, the decay follows closely a monoexponential form, thus, a recombination rate constant can be extracted from a slope of a semilogarithmic plot.[15]

Results and discussion

Synthesis

The target compound was obtained from a series of three reactions as shown in Scheme 1. A reaction of the tetracarboxylic acid **1**[10] with NHS and EDC·HCl yielded ester **2** which immediately reacted with diacetylene **3**,[11] due to its hygroscopicity, to afford compound **4**. The formation of compound **4** was confirmed by the presence of its molecular peak at m/z 1817.311 on a MALDI-TOF mass spectrum corresponding to its molecular mass, and characteristic patterns of free base porphyrin on its absorption and emission spectra.
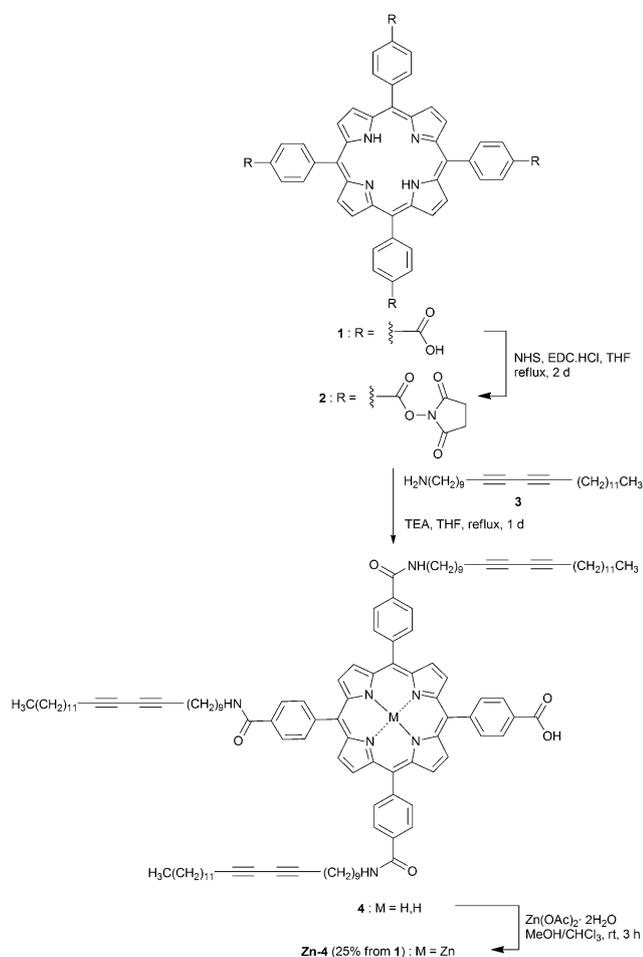
A subsequent Zn-metallation of compound **4** with $Zn(OAc)_2 \cdot 2H_2O$ gave **Zn-4** in 25% overall yield. The completion of the metallation step was indicated by the absence of an emission peak at 712 nm and a ^{1}H-NMR peak of the inner protons at about $\delta -2$ ppm in the spectra of compound **Zn-4**. The solubility of **Zn-4** was found to be more than 20 mg mL^{-1} in common organic solvents, $e.g.$ CH$_2$Cl$_2$, CHCl$_3$, and THF, which is sufficient for a routine wet process in DSSC fabrication.

Photophysical and electrochemical properties

The photophysical properties, namely absorption as a function of a wavelength of an incident light, were determined for the monomer solution and the polymer film. The resulting curves are presented in Fig. 1. The UV-vis absorption spectra of a **Zn-4** solution in toluene exhibited a characteristic pattern of Zn-porphyrin having a B-band at 425 nm, and Q-bands at 557 and 598 nm (black solid line). A **poly-Zn-4** film, prepared by the 254 nm ultraviolet radiation of a **Zn-4**-coated TiO$_2$ film at room temperature for 15 min, gave the similar absorption pattern with slightly broader bands and higher intensity of the first Q-band (red dashed line). The broadening of the absorption bands can be explained by the possible macrocycle aggregation. Although the film was relatively thin on the TiO$_2$ surface, the enhancement of the Q-band, possibly resulted from the co-absorption of the PDA formed in the film, can be seen. These results are in a good agreement with our previous report.[7]

The electrochemical properties of the **poly-Zn-4** film on the ITO/glass glass substrate were studied by cyclic voltammetry. Results revealed that the **poly-Zn-4** film can be both electrochemically oxidized and reduced (Fig. 2). In the oxidation domain (Fig. 2a, black solid line), two quasireversible anodic peaks of **poly-Zn-4** were observed at the peak potentials of +0.7 V and +1.3 V, related to two successive one-electron oxidation processes. Due to the dissolvation of the film into the electrolyte solution during the measurement, the positive scanning was not performed beyond the potential of +1.5 V. Compared with 5-(4-carboxyphenyl)-10,15,20-(triphenyl)porphinatozinc(II) (**ZnTPP-COOH**; Fig. 2a, red dashed line), it was observed that the first oxidation of **poly-Zn-4** occurred in the similar potential (+0.7 V $vs.$ +0.8 V), while the second oxidation of **poly-Zn-4** occurred at 0.2 V higher potential (+1.3 V $vs.$ +1.1 V).

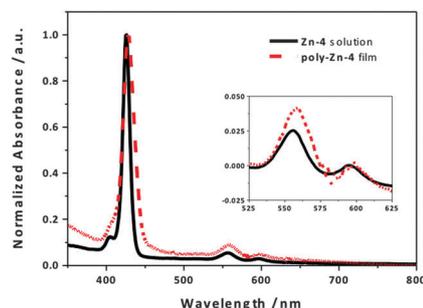**Scheme 1** Synthesis of the target compound.

Fig. 1 Absorption spectra of a **Zn-4** solution in toluene (black solid line) and a **poly-Zn-4** film (red dashed line). The inset shows a magnification of the region between 525 and 625 nm with baseline calibration for a comparison purpose.
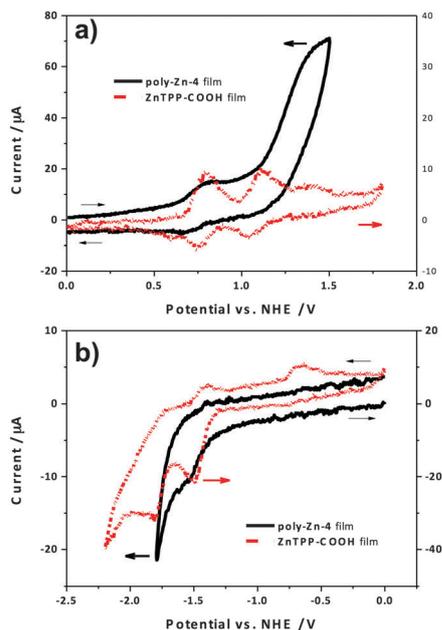
Fig. 2 Cyclic voltammograms of a **poly-Zn-4** film in the ranges between (a) 0 and +1.5 V and (b) 0 and −1.8 V in comparison with those of **ZnTPP-COOH** film in the ranges between (a) 0 and +1.8 V and (b) 0 and −2.2 V.

In the reduction process of **poly-Zn-4** (Fig. 2b), the dissolvation of the film was observed beyond the potential of −1.8 V, and therefore the measurement was carried out from 0.0 V to −1.8 V (Fig. 2b, black solid line). In this region, **poly-Zn-4** gave one irreversible peak at −1.5 V, which is corresponding to the first cathodic potential of **ZnTPP-COOH** (−1.5 V; Fig. 2b, red dashed line). In the case of **ZnTPP-COOH**, the second cathodic signal was observed at −1.8 V with the indefinable anodic signal from −0.4 and −0.8 V. This is likely to be resulted from the possible formation of unknown products from the reduction process(es) of **ZnTPP-COOH**, which is attributed to the molecular cleavage, as this feature was more conspicuous at higher cycle numbers. In comparison with the results obtained from **ZnTPP-COOH**, these small shifts of redox potentials and the film instability observed from **poly-Zn-4** film indicate a significant effect of the presence of the PDA-containing alkyl chains on the electrochemical characteristics of the porphyrin ring.

Following previous studies,[16] a highest occupied molecular orbital (HOMO) energy level of a dye can be represented by its $E_{1/2}$ value of the first oxidation or $E_{1/2}(ox1)$, while a lowest unoccupied molecular orbital (LUMO) energy level can be estimated from an excited state oxidation potential $(E_{0-0}{}^\star)$ by the following equation:

$$E_{0-0}{}^\star = E_{1/2}(ox1) - E_{0-0}$$

where E_{0-0} is an absorption onset of the dye. Since **poly-Zn-4** was obtained in the form of a film, the values from the above-mentioned cyclic voltammetry measurements were used in this calculations. The results revealed that **poly-Zn-4** were found to have an energy gap of 2.0 V with the LUMO and HOMO energy levels of −1.3 and +0.7 V, respectively. With the LUMO energy

level being more negative than the conduction band of TiO_2 (−0.50 V *vs.* NHE) and the HOMO energy level more positive than the oxidation potential of an iodide ion/triiodide ion $(I^-/I_3{}^-)$ redox couple (+0.40 V *vs.* NHE), the electron injection of the excited dye to the TiO_2 surface and the dye regeneration by the $I^-/I_3{}^-$ electrolyte should be thermodynamically possible in the DSSCs based on **poly-Zn-4**.

Photovoltaic characteristics. The **poly-Zn-4**-based solar cells were assembled using a double layer TiO_2 film (8 + 5 μm) in conjugation with an acetonitrile-based electrolyte solution. A detailed description is given in the Device fabrication section. Fig. 3 shows the photovoltaic performance of the devices under standard AM 1.5 G 1000 W m^{-2} illumination. From the current–voltage (*J–V*) curve shown in Fig. 3a, the best **poly-Zn-4**-based solar cell exhibited, respectively, a short-circuit photo-current density (J_{sc}), an open-circuit voltage (V_{oc}) and a fill factor (FF) of 4.2 mA cm^{-2}, 0.7 V and 0.78, respectively, which yielded an overall power conversion efficiency (PCE) value of 2.3%. It is important to note that the PCE was increased by 35% of the original value (from 1.7% to 2.3%) when the device was illuminated under the standard AM 1.5 G 1000 W m^{-2} light intensity for ~40 minutes before the *J–V* measurement was performed. According to the previous study,[17] the substitution of the DA-containing alkyl chains in the *meso*-phenyl groups of the porphyrin ring resulted in retardation of the charge recombination processes and enhanced the interfacial charge separation. Moreover, compared with the previous study of **ZnTPP-COOH**-based DSSCs,[18] the PDA-containing alkyl chains in **poly-Zn-4** resulted in a remarkable increase in PCE value (1.8% *vs.* 2.3%). This phenomenon could be attributed to the solid-state photo-induced PDA formation in the **poly-Zn-4** film,
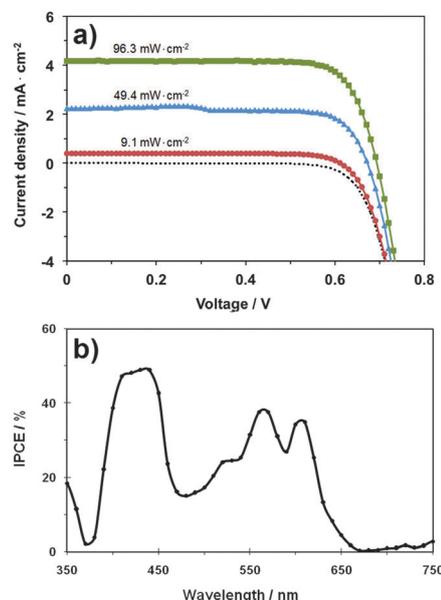

Fig. 3 (a) Current density−voltage curves of the **poly-Zn-4**-based solar cell under simulated solar irradiation of 96.3 (green solid line), 49.4 (blue solid line) and 9.1 (red solid line) mW cm^{-2} (AM 1.5), and in the dark (black dotted line); and (b) IPCE spectrum of the **poly-Zn-4**-based solar cell.

leading to the increase in the number of π-conjugation network and, as a result, raising the light harvesting efficiency of the dye. However, a relatively low value of PCE might have resulted from the porphyrin aggregation on the TiO₂ surface as indicated by the broadened absorption bands of the **poly-Zn-4** film on TiO₂. A similar observation has also been found in the case of **ZnTPP-COOH**.[18] The aggregation can cause the quenching processes of the excited states to the adjacent porphyrin units, subsequently increasing unfavorable charge recombination processes and reducing the electron injection efficiency.[19]

The corresponding IPCE spectrum of the **poly-Zn-4**-based solar cell is shown in Fig. 3b. The pattern of the IPCE spectrum is consistent with the absorption spectra of the **Zn-4** solution and the **poly-Zn-4** film with the IPCE values at 430, 570 and 610 nm of 48.9% and 37.6% and 34.8%, respectively. In addition, the presence of the PDA network in the case of **poly-Zn-4** significantly increased the ratio of the long-wavelength peaks to the short-wavelength peak in the IPCE spectrum (0.77 and 0.71 for the peaks at 570 and 610 nm, respectively) compared to that of **ZnTPP-COOH** (approximately 0.3 and 0.2, excerpted from ref. 18). This suggested an enhancement in the light harvesting efficiency in the visible region of **poly-Zn-4** bound to the TiO₂ surface resulting from the PDA-containing C₂₅ alkyl units.

To further investigate the electron recombination between rate **poly-Zn-4** and TiO₂ nanoparticles, the transient photovoltage decay measurement was performed. The decay of the recombination lifetime exhibits an exponential dependence with respect to the photovoltage under open-circuit conditions as shown in Fig. 4. It appeared that the electron lifetime became shorter as more charges were injected from the excited states of **poly-Zn-4** into the conduction band of TiO₂ nanoparticles, leading to the faster reaction of electrons and I_2^- species in the electrolyte when the solar cell was exposed to the light at stronger intensity. The electron lifetime of the **poly-Zn-4**-based solar cell at 0.60 V was approximately 40 ms, which is twice longer than the value of 21.2 ms that was reported for **ZnTPP-COOH**.[18] We attribute this effect to the substitution of PDA-containing C₂₅ alkyl chains in the *meso*-phenyl groups of the porphyrin ring. Furthermore, the chemical capacitance (C_μ) of the **poly-Zn-4**-based solar cell increased exponentially with

an increasing bias potential under open-circuit conditions. It is also suggested that the chemical capacitance dependence on V_{oc} follows an exponential law as $C_\mu \propto \alpha q V_{oc}/k_B T$ with $\alpha = 0.34$.

Conclusions

The target diacetylene–porphyrin monomer was successfully prepared and showed satisfactory solubility characteristics. The formation of the polydiacetylene–nested zinc-porphyrin was indicated by the slight enhancement of the absorption in the Q-band region relative to the monomer. The results from cyclic voltammetry showed that the polydiacetylene–nested zinc-porphyrin exhibited the suitable levels of the highest occupied molecular orbital and the lowest unoccupied molecular orbital for use in dye-sensitized solar cells. Device studies suggested that the incorporation of the polydiacetylene network and the porphyrinic system was advantageous for the device performance with respect to the previously reported system based on 5-(4-carboxyphenyl)-10,15,20-(triphenyl)porphinatozinc(II).

Acknowledgements

References

1 K. M. Kadish, E. V. Caemelbecke and G. Royal, in *The Porphyrin Handbook*, ed K. M. Kadish, K. M. Smith and R. Guilard, Academic Press, New York, 2000, vol. 8, ch. 55.

2 Selected publications: (*a*) K. Kalyanasundaram, N. Vlachopoulos, V. Krishnan, A. Monnier and M. Grätzel, *J. Phys. Chem.*, 1987, **91**, 2342; (*b*) A. Kay and M. Grätzel, *J. Phys. Chem.*, 1993, **97**, 6272; (*c*) D. Wohrle, B. Tennigkeit, J. Elbe, L. Kreienhoop and G. Schurpfeil, *Mol. Cryst. Liq. Cryst.*, 1993, **230**, 221; (*d*) S. Cherian and C. C. Wamser, *J. Phys. Chem. B*, 2000, **104**, 3624; (*e*) F. Odobel, E. Blart, M. Lagree, M. Villieras, H. Boujtita, N. El Murr, S. Caramori and C. A. Bignozzi, *J. Mater. Chem.*, 2003, **13**, 502; (*f*) W. M. Campbell, A. K. Burrell, D. L. Officer and K. W. Jolly, *Coord. Chem. Rev.*, 2004, **248**, 1363; (*g*) H. Imahori, *J. Phys. Chem. B*, 2004, **108**, 6130; (*h*) T. Hasobe, P. V. Kamat, M. A. Absalom, Y. Kashiwagi, J. Sly, M. J. Crossley, K. Hosomizu, H. Imahori and S. Fukuzumi, *J. Phys. Chem. B*, 2004, **108**, 12865; (*i*) Q. Wang, W. M. Campbell, E. E. Bonfantani, K. W. Jolley, D. L. Officer, P. J. Walsh, K. Gordon, R. Humphry-Baker, M. K. Nazeeruddin and M. Grätzel, *J. Phys. Chem. B*, 2005, **109**, 15397; (*j*) T. Hasobe, S. Fukuzumi and P. V. Kamat, *J. Phys. Chem. B*, 2006,
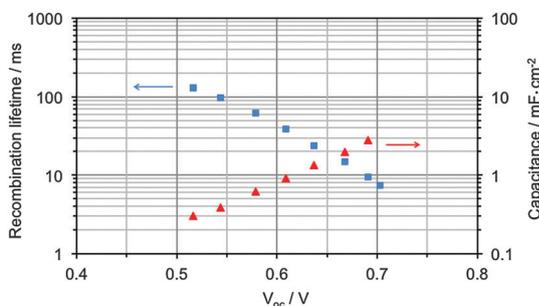

Fig. 4 Plots of electron recombination lifetime (blue square) and chemical capacitance (red triangle) *vs.* open-circuit voltage of the **poly-Zn-4**-based solar cells.

110, 25477; (*k*) W. M. Campbell, K. W. Jolly, P. Wagner, K. Wagner, P. J. Walsh, K. C. Gordon, L. S. Mende, M. K. Nazeerruddin, Q. Wang, M. Grätzel and D. L. Officer, *J. Phys. Chem. C*, 2007, **111**, 11760; (*l*) H. Imahori, T. Umeyama and S. Ito, *Acc. Chem. Res.*, 2009, **42**, 1809; (*m*) R. M. Ma, P. Guo, H. J. Cui, X. X. Zhang, M. K. Nazeerruddin and M. Grätzel, *J. Phys. Chem. A*, 2009, **113**, 10119.

3 Selected publications: (*a*) M. A. Baldo, D. F. O'Brien, Y. You, A. Shoustikov, S. Sibley, M. E. Thompson and S. R. Forrest, *Nature*, 1998, **395**, 151; (*b*) R. C. Kwong, S. Sibley, T. Dubovoy, M. Baldo, S. R. Forrest and M. E. Thompson, *Chem. Mater.*, 1999, **11**, 3709; (*c*) T. F. Guo, S. C. Chang, Y. Yang, R. C. Kwong and W. E. Thompson, *Org. Electro-chem.*, 2000, **1**, 15; (*d*) E. M. Gross, N. R. Armstrong and R. M. Wightman, *J. Electrochem. Soc.*, 2002, **149**, E137; (*e*) V. A. Montes, C. Perez-Bolivar, N. Agarwal, J. Shinar and P. Anzenbacher, *J. Am. Chem. Soc.*, 2006, **128**, 12436; (*f*) X. Wang, H. Wang, Y. Yang, Y. He, L. Zhang, Y. Li and X. Li, *Macromolecules*, 2010, **43**, 709.

4 Selected publications: (*a*) Y. Y. Noh, K. Yase and S. Nagamatsu, *Appl. Phys. Lett.*, 2003, **83**, 1243; (*b*) Y. Y. Noh, J. J. Kim, Y. Yoshida and K. Yase, *Adv. Mater.*, 2003, **15**, 699; (*c*) P. Checcoli, G. Conte, S. Salvatori, R. Paolesse, A. Bolognesi, A. Berliocchi, F. Brunetti, A. D'Amico, A. Di Carlo and P. Lugli, *Synth. Met.*, 2003, **138**, 261; (*d*) P. B. Shea, J. Kanicki and N. Ono, *J. Appl. Phys.*, 2005, **98**, 014503; (*e*) C.-M. Che, H.-F. Xiang, S. S.-Y. Chui, Z.-X. Xu, V. A. L. Roy, J. J. Yan, W.-F. Fu, P. T. Lai and I. D. Williams, *Chem. – Asian J.*, 2008, **3**, 1092; (*f*) X. B. Huang, C. L. Zhu, S. M. Zhang, W. W. Li, Y. L. Guo, X. W. Zhan, Y. Q. Liu and Z. Z. Bo, *Macromolecules*, 2008, **41**, 6895; (*g*) P. Ma, Y. Chen, X. Cai, H. Wang, Y. Zhang, Y. Gao and J. Jiang, *Synth. Met.*, 2010, **160**, 510.

5 (*a*) A. Yella, H.-W. Lee, H. N. Tsao, C. Yi, A. K. Chandiran, M. K. Nazeerruddin, E. W.-G. Diau, S. M. Zakeeruddin and M. Grätzel, *Science*, 2011, **334**, 629; (*b*) S. Mathew, A. Yella,

P. Gao, R. Humphry-Baker, B. F. E. Curchod, N. Ashari-Astani, I. Tavernelli, U. Rothlisberger, M. K. Nazeeruddin and M. Grätzel, *Nat. Chem.*, 2014, **6**, 242.

6 (*a*) Mitsubishi Chemical Holdings Corporation, http://www.m-kagaku.co.jp/english/aboutmcc/RC/special/feature1.html, accessed April 17, 2012; (*b*) R. F. Service, *Science*, 2011, **332**, 293.

7 C. Reanprayoon, J. Gasiorowski, M. Sukwattanasinitt, N. S. Sariciftci and P. Thamyongkit, *RSC Adv.*, 2014, **4**, 3045.

8 M. Shirakawa, N. Fujita and S. Shinkai, *J. Am. Chem. Soc.*, 2006, **127**, 4164.

9 Y. P. Wang, K. Yang, X. Y. Wang, R. Nagarajan, L. A. Samuelson and J. Kumar, *Org. Electron.*, 2006, **7**, 546.

10 A. D. Adler, F. R. Longo, J. D. Finarelli, J. Goldmacher, J. Assour and L. Korsakoff, *J. Org. Chem.*, 1967, **32**, 476.

11 N. M. Howarth, W. E. Lindsell, E. Murray and P. N. Preston, *Tetrahedron*, 2005, **61**, 8875.

12 S. J. Kew and E. A. H. Hall, *J. Mater. Chem.*, 2006, **16**, 2039.

13 J. Jiao, P. Thamyongkit, I. Schmidt, J. S. Lindsey and D. F. Bocian, *J. Phys. Chem. C*, 2007, **111**, 12693.

14 P. Wang, M. Zakeeruddin, P. Comte, R. Charvet, R. Humphry-Baker and M. Grätzel, *J. Phys. Chem. B*, 2003, **107**, 14336.

15 M. Wang, X. Li, H. Lin, P. Pechy, S. M. Zakeeruddin and M. Grätzel, *Dalton Trans.*, 2009, 10015.

16 (*a*) D. P. Hagberg, J.-H. Yum, H. Lee, F. D. Angelis, T. Marinado, K. M. Karlsson, R. Humphry-Baker, L. Sun, A. Hagfeldt, M. Grätzel and M. K. Nazeeruddin, *J. Am. Chem. Soc.*, 2008, **130**, 6259; (*b*) J. K. Park, H. R. Lee, J. Chen, H. Shinokubo, A. Osuka and D. Kim, *J. Phys. Chem. C*, 2008, **112**, 16691.

17 S. M. Feldt, E. A. Gibson, E. Gabrielsson, L. Sun, G. Boschloo and A. Hagfeldt, *J. Am. Chem. Soc.*, 2010, **132**, 16714.

18 H. He, A. Gurung and L. Si, *Chem. Commun.*, 2012, **48**, 5910.

19 M. R. Viseu, G. Hungerford and M. I. C. Ferreira, *J. Phys. Chem. B*, 2002, **106**, 1853.